Development of an Impact Capability for the Three-Dimensional Fluid-Structure Interaction Code — NEPTUNE

R.F. Kulak, C. Fiala

Argonne National Laboratory, Reactor Analysis and Safety Division, 9700 South Cass Ave., Argonne, Illinois 60439, U.S.A.

Abstract

A method, which uses a family of adaptive contact elements, is developed for treating the mechanics of contact/impact between two deformable bodies. The contact element's nodal connectivity is allowed to change during the computations in order to accommodate finite sliding. The methodology has been implemented into the NEPTUNE finite element program. Results are presented for an illustrative problem.

1. Introduction

NEPTUNE [1] is a three-dimensional, finite-element based computer program developed by Argonne National Laboratory for the transient analysis of reactor safety problems that involve structures, fluids, or fluid-structure interactions. Recent involvement in liquid metal fast breeder reactor (LMFBR) structural safety problems has lead to a need for an efficient three-dimensional contact/impact methodology. In particular, we are primarily concerned with the contact/impact mechanics that occur during slug impact (1) at the plug-to-plug junctures in a triple rotatable plug type of head closure, (2) between the shield plates of the head closure, and (3) at the sodium-head interface. The development of a family of contact elements that can be used to simulate the mechanics of gap-impact is presented here.

2. Interface Mechanics

Consider two surfaces, S_1 and S_2, to have a common interface (i.e., a contact interface), S_c, given by $S_c=S_1 \cap S_2$. When contact occurs, the normal tractions, σ_n, and normal velocities, v_n, are given by

$$\sigma_n^1 + \sigma_n^2 = 0 \; ; \qquad v_n^1 = v_n^2 \qquad \text{on } S_c \; , \tag{1}$$

where the superscripts 1 and 2 indicate surface 1 and 2, respectively. Since adhesion is not allowed at the interface, only negative normal tractions are permitted. Also, the surfaces are not permitted to penetrate into each other; thus

$$\sigma_n \leq 0 \; ; \qquad g = h-h_c \geq 0 \qquad \text{on } S_c \; , \tag{2}$$

where g is the gap normal to the interface, h is the current height of the element, and h_c is the height of the element when contact occurs. Pires and Oden [2] pointed out that the addition of the penalty term $\sigma_n g_n$ to the total energy of the system is equivalent to replacing the contact conditions, Eq. (2), by the relation

$$\sigma_n = -\frac{1}{\delta} g \,, \tag{3}$$

where δ is the penalty parameter. Therefore, we can satisfy the unilateral contact condition, in a weak sense, by infusing the interface with finite elements that have Eq. (3) as their traction-gap relation.

Once contact occurs, frictional tractions, σ_t, will develop in the direction of the relative velocity (i.e., sliding), $\dot{s}$, between the two surfaces.

In order to obtain an equivalent set of nodal forces from the distributions of σ_n and σ_t over the contact surface, we employed the principal of virtual power

$$\int_{S_c} \sigma_n \dot{g} \, dS_c = f^n_{iI} v_{iI} \; ; \qquad \int_{S_c} \sigma_t \dot{s} \, dS_c = f^t_{iI} v_{iI} \,, \tag{4}$$

where f^n_{iI} and f^t_{iI} are the components of the nodal force due to the normal and tangential tractions, respectively, at node I in the ith global coordinate direction, and $\dot{v}_{iI}$ are the components of velocity. Now we will assume that the rate-of-change in gap, $\dot{g}$, and the sliding velocity, $\dot{s}$, can be expressed in linear forms given by

$$\dot{g} = B^n_{iI} \, v_{iI} \; ; \qquad \dot{s} = B^t_{iI} \, v_{iI} \,, \tag{5}$$

where B^n_{iI} and B^t_{iI} are to be determined. Using Eqs. (4) and (5) and noting the arbitrariness of the nodal velocities, the internal forces were found to be

$$f^n_{iI} = \int_{S_c} \sigma_n B^n_{iI} \, dS_c \; ; \qquad f^t_{iI} = \int_{S_c} \sigma_t B^t_{iI} \, dS_c \,. \tag{6}$$

The normal and tangential tractions are computed from appropriate constitutive equations.

3. Contact/Impact Elements

It was determined that a family of three elements was needed in order to handle all the possible configurations that can occur between the discretized contacting bodies: a tetrahedral element, a triangular element, and a line element. However, because of space limitations, we will only treat the highlights of the development of the tetrahedral element.

It will be helpful to define an interface vector triad ($\underset{\sim}{n}$, $\underset{\sim}{t}_1$, $\underset{\sim}{t}_2$) for each contact element such that $\underset{\sim}{n}$ is normal to the base, $\underset{\sim}{t}_1$ is tangent to the base and in the direction of sliding, and $\underset{\sim}{t}_2$ is also tangent to the base and orthogonal to $\underset{\sim}{n}$ and $\underset{\sim}{t}_1$. The rate-of-change in gap, $\dot{g}$, is measured along $\underset{\sim}{n}$, and the sliding velocity, $\dot{\underset{\sim}{s}}$, is measured along $\underset{\sim}{t}_1$.

Since we always position the tetrahedron so that nodes 1, 2, and 3 (Fig. 1) lie on one impacting surface and node 4 lies on the other, we see that the height is measured from the base formed by nodes 1-2-3 to the apex at node 4. The height and rate-of-change in element height are given, respectively, by

$$h = 3V/A \; ; \qquad \dot{h} = B_{kI} v_{iI} \; , \tag{7}$$

where V is the volume of the tetrahedron, A is the area of the base, and B_{iI} is a matrix which must be determined for each element. This form for the rate-of-change of element height was used by Kennedy and Belytschko [3] for two dimensional geometries. The coefficients, B_{iI}, for the base nodes of the tetrahedron (i.e., I = 1, 2, 3) are given by

$$B_{iI} = \frac{0.5}{A_{123}} (x_{jJ} x_{k4K} + x_{jK} x_{kJ4} + x_{j4} x_{kKJ}) - \frac{1.5V}{A_{123}^3} (A_j x_{kKJ} + A_k x_{jJK}) \; , \tag{8a}$$

and for the apex node (i.e., I = 4) by

$$B_{i4} = \frac{0.5}{A_{123}} (x_{j1} x_{k23} + x_{j3} x_{k12} + x_{j2} x_{k31}) \; , \tag{8b}$$

where, for example, x_{kKJ} is defined to be the difference between the kth coordinate of nodes K and J. The appropriate node numbers are given in the permutation table (Table I). The subscripts (i,j,k) take cyclical permutations of (x,y,z). A_{123} is the area of face 1-2-3, A_j is the projected area in the jth direction.

The sliding velocity between the base and apex of the element is taken to be the difference between the tangential velocity of the apex minus the average tangential velocity of the base. The relative sliding, expressed in the interface coordinate system, is given by

$$\dot{s} = \hat{B}_{iI}^t \; \hat{v}_{iI} \; , \tag{9}$$

where

$$\{\hat{B}^t\}^T = [0 \;\; -\tfrac{1}{3} \;\; 0 \;\; 0 \;\; -\tfrac{1}{3} \;\; 0 \;\; 0 \;\; -\tfrac{1}{3} \;\; 0 \;\; 0 \;\; 1 \;\; 0] \; , \tag{10}$$

$$\{\hat{v}\}^T = [\hat{v}_{n1} \;\; \hat{v}_{t_1 1} \;\; \hat{v}_{t_2 1} \;\; \hat{v}_{n2} \;\; \hat{v}_{t_1 2} \;\; \hat{v}_{t_2 2} \;\; \hat{v}_{n3} \;\; \hat{v}_{t_1 3} \;\; \hat{v}_{t_2 3} \;\; \hat{v}_{n4} \;\; \hat{v}_{t_1 4} \;\; \hat{v}_{t_2 4}] \; , \tag{11}$$

and the "^" symbol is used to indicate that the components are expressed in the local coordinate system. The nodal forces due to sliding are given in the local coordinate system by

$$\hat{f}_{iI}^t = A_{123} \; \sigma^t \; \hat{B}_{iI}^t \; . \tag{12}$$

Global components for the nodal forces are obtained through standard coordinate transformation procedures.

4. Adaptive Connectivity

During the discretization of a problem potential contact elements are defined. Each of these elements consists of a base and an apex node. The specific node(s) that form the base of the element are defined by the user and remain fixed throughout the numerical simulation. In contrast, the apex node of the element can be associated with different contact elements at different times during the simulation.

In order to reduce the computational time required when a search is performed to identify the element that an apex node is associated with, we utilized a contact element adjacency table. For each tetrahedral contact element, the table contains the element numbers of all the contiguous tetrahedral contact elements. Thus, when a specific apex node fails to project itself onto the base that it was previously identified with, the adjacency table contains the information needed to reconnect the apex node to another base.

At the end of each computational cycle, the connectivity of all the tetrahedral contact elements are checked to see if their apex nodes continue to project onto their previous bases. The node projection is performed in the following manner. The three in-plane, edge normals (Fig. 2) are given by

$$\underset{\sim}{N}_{12} = \underset{\sim}{n} \times \underset{\sim}{L}_{12} \; ; \qquad \underset{\sim}{N}_{23} = \underset{\sim}{n} \times \underset{\sim}{L}_{23} \; ; \qquad \underset{\sim}{N}_{31} = \underset{\sim}{n} \times \underset{\sim}{L}_{31} \; , \tag{13}$$

Marti [4] has stated that necessary and sufficient conditions for a node to project within the triangle are

$$\underset{\sim}{L}_{14} \cdot \underset{\sim}{N}_{12} > 0 \; ; \qquad \underset{\sim}{L}_{24} \cdot \underset{\sim}{N}_{23} > 0 \; ; \qquad \underset{\sim}{L}_{34} \cdot \underset{\sim}{N}_{31} > 0 \; . \tag{14}$$

When all three of the above inequalities are fulfilled, the apex node projects onto its triangular base and the element connectivity remains unchanged. However, if one of them fails then the apex node is no longer connected to this element and a search is made, using the information from the adjacency table, to find its new projection and reconnection.

5. Example

To illustrate the use of the above methodology, we simulated the response of a cladded cylinder impacting against a rigid floor. This problem was one of the benchmark calculations for the impact response of casks containing nuclear waste reported by Yagawa et al. [5]. Figure 3 is a schematic view of the problem. A 914 mm long lead cylinder with a 305 mm diameter is dropped from a height of 9.0 m onto a rigid floor. The cylinder is clad with 6.35 mm thick stainless steel. At impact the velocity of the cask is 13,330 mm/s, which is the free fall velocity. The material properties for the lead and steel are listed in Table II. A bilinear stress-strain representation is employed for both the steel and lead. Figure 4 shows an elevation view of our finite element model. The cylinder is modelled with 8-node hexahedrons, and the cladding is modelled with 3-node triangular plate elements. The following boundary conditions were applied to the problem. After impact the base of the cask was constrained to remain against the floor. This condition was chosen only to be consistant with the models reported by Yagawa et al. [5]. Contact elements were located between the cylinder and its cladding in order to allow sliding and possible separation at the interface.

Figure 5 shows the history of the head settlement, which is the displacement of the top of the lead cylinder. The cask impacts against the floor at 0.0 ms. The maximum calculated value for head settlement was 6.5 cm and occurred at 5.5 ms. Yagawa [5] reported on the results from several organizations, which used different computer programs. The range for maximum head settlement and the time at which it occurred for three out of four of the calculations of Ref. [5] was 5.8 to 7.25 cm and 4.3 to 6.25 m, respectively; the fourth calculation was significantly out of the above ranges. Our results compare favorably with the above ranges.

6. Acknowledgments

The authors wish to thank Drs. S. H. Fistedis and J. M. Kennedy for their support. This work is part of the Engineering Mechanics Program of the Reactor Analysis and Safety Division of Argonne National Laboratory and was supported by the U.S. Department of Energy.

References

[1] KULAK, R. F., FIALA, C., "A Lagrangian Three-Dimensional Finite-Element Formulation for the Nonlinear Fluid-Structural Response of Reactor Components," ANL-80-26 (March, 1980).

[2] PIRES, E. B., ODEN, J. T., "Analysis of Contact Problems with Friction Under Oscillating Loads," Comp. Meth. in Appl. Mech. and Eng., 39, 337-362 (1983).

[3] KENNEDY, J. M., BELYTSCHKO, T. B., "Buckling and Post-Buckling Behavior of the ACS Support Columns," Nuclear Engineering and Design, 75 (3), 323-342 (1983).

[4] MARTI, J., "PR3D Documentation Manual," Tech. Rpt. No. PR-TN-4.32, Principia Mechanica Ltd., London, UK (June, 1983).

[5] YAGAWA, G., OHTSUBO, H., TAKEDA, H., TOI, Y., AIZAWA, T., IKUSHIMA, T., "A Round Robin on Finite Element Calculation for Impact Problems," Nuclear Engineering and Design, 78(3), pp. 377-388 (1984).

Table I. Permutation Table

I	J	K
1	2	3
2	3	1
3	1	2

Table II. Material Properties

	Lead	Stainless Steel
Density, Kg sec^2/mm^4	1.13×10^{-9}	8.0×10^{-10}
Young's Modulus, Kg/mm^2	19.5	1.96×10^4
Poisson's Ratio	0.42	0.33
Yield Stress, Kg/mm^2	3.02	31.6
Tangent Modulus, Kg/mm^2	1.85	195.0

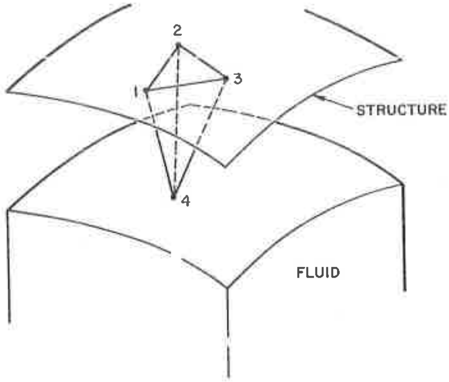

Fig. 1. Typical Interface with a Tetrahedral Contact/Impact Element

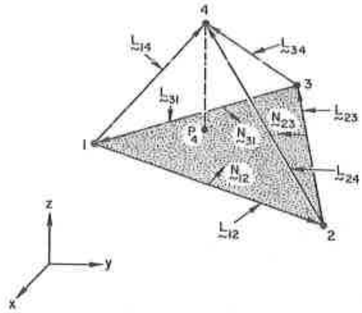

Fig. 2. Vectors Used in Adaptive Connectivity Scheme for the Tetrahedron

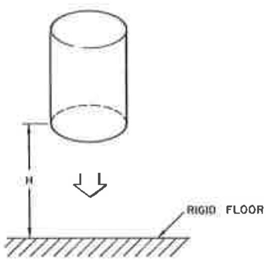

Fig. 3. Cladded Cylinder Impacting Against a Rigid Floor

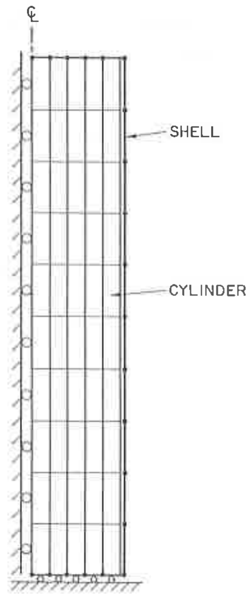

Fig. 4. Elevation View of Finite Element Model for Impacting Cylinder

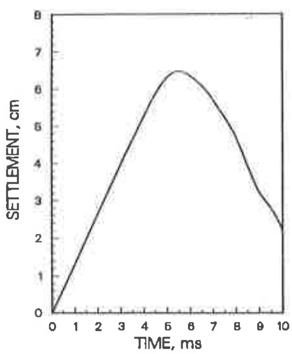

Fig. 5. Temporal History of Head Settlement as Predicted by NEPTUNE